PCCP

Accepted Manuscript

This is an *Accepted Manuscript*, which has been through the Royal Society of Chemistry peer review process and has been accepted for publication.

Accepted Manuscripts are published online shortly after acceptance, before technical editing, formatting and proof reading. Using this free service, authors can make their results available to the community, in citable form, before we publish the edited article. We will replace this *Accepted Manuscript* with the edited and formatted *Advance Article* as soon as it is available.

You can find more information about *Accepted Manuscripts* in the Information for Authors.

Please note that technical editing may introduce minor changes to the text and/or graphics, which may alter content. The journal's standard Terms & Conditions and the Ethical guidelines still apply. In no event shall the Royal Society of Chemistry be held responsible for any errors or omissions in this *Accepted Manuscript* or any consequences arising from the use of any information it contains.

ROYAL SOCIETY OF CHEMISTRY

www.rsc.org/pccp

Please do not adjust margins

Journal Name

ARTICLE

Excited-State Localization and Energy Transfer in Pyrene Core Dendrimers with Fluorene/ Carbazole as Dendrons, and Acetylene as Linkages

Received 00th January 20xx,
Accepted 00th January 20xx

DOI: 10.1039/x0xx00000x

www.rsc.org/

Linyin Yan,*[ab] Yan Wan,[ab] Andong Xia ,[ab] ShengHien Lin*[c] and Ran Huang[d]

A multi-leveled theoretical investigation combining TD-DFT(B3LYP and CAM-B3LYP) methods and semi-empirical method has been conducted to determine the structure-related spectral properties for T-series dendrimers composed of nearly hundreds of atoms, which has been carried outbased on the proposed molecular model. Both one- and two-photon absorption spectra of these dendrimer molecules have been well reproduced. The "antenna effect" in the dendrimers molecule has been theoretically studied. The process of excitation energy localization from chromophores in branches to the pyrene core before the fluorescence emission is visualized by using the contour of charge different density (CDD) between electronic states. The conclusions based on the theoretical model have been drawn to the observed photophysical properties of T-series dendrimers: a). increasing a generation of branch would enhance the absorption of photons with wavelength below 430 nm; b). enlarging the conjugation of branches would enhance the coupling among the chromophores and lower the excitation energy; c). the existence of inter-molecular coupling among the "antenna" chromophores in conjugated branches and the pyrene core would significantly promote two photons absorption.

1 Introduction

The dendritic structure is considered as one of the promising structures to design two-photon absorption (2PA) materials with large 2PA cross section and highly efficient two-photon excited fluorescence (TPEF)[1-12]. Two mainly unique features of the dendritic structure, called "antenna effect" and "shell effect", would guarantee outstanding photophysical properties[8, 9, 13, 14]. In order to design and determine structure-dependent 2PA properties of dendrimers, both the theoretical and applied researches related to dendrimers have been mushrooming in recent years. Great efforts have been taken to synthesize new dendrimers and modify the existing ones[4-6, 15-17]. Theoretical investigations have also been carried out to explain the experimental results, and a number of factors have been found to have effects on the 2PA of dendrimers, such as electronic delocalization, degree of molecular planarity, cooperative enhancement between chromophores, and so on[2, 5-8, 10, 18-31]. Hereon, theoretical models for dendrimers should be built to quantitatively describe the structure-property relationship, and effectively guide the dendrimer designing. Unfortunately, since many dendrimers reported to have excellent 2PA properties contains hundreds of atoms[8, 12, 14, 32-34], the large size of dendrimer molecules makes the single-scaled modeling with TD-DFT calculation not applicable. Exciton models or other models should be employed to divide the dendrimer molecule into several parts, so that the theoretical method for smaller molecules could be applicable for large dendrimers.[35-42 35-42]

In order to obtain a comprehensive understanding of the structure-related properties of the excited states in dendrimers and their impact on the molecular photophysical properties, in this paper, a multi-leveled theoretical investigation contains compatible TD-CAM-B3LYP and ZINDO calculation have been conducted on a series of T-series dendrimers (the molecular structures of **T1-T4** are shown in Scheme 1)[43]. A multi-scaled accurate theoretical model has been established, which could quantitatively reproduce one- and two-photon absorption properties, and the corresponding new designing strategies for such type of dendrimers are proposed.

[a] *The State Key Laboratory of Molecular Reaction Dynamics, Institute of Chemistry, Chinese Academy of Sciences, Beijing 100190, P. R. China. E-mail: yanlinyin@iccas.ac.cn; Tel: +86-13810491497.*
[b] *Beijing National Laboratory for Molecular Sciences (BNLMS), Institute of Chemistry, Chinese Academy of Sciences, Beijing 100190, P. R. China*
[c] *Department of Applied Chemistry, National Chiao Tung University, Hsinchu, Taiwan 30010, China. E-mail: sheng@mail.nctu.edu.tw.*
[d] *School of Chemistry and Chemical Engineering, Shanghai Jiao Tong University, Shanghai 200240, China*
† Electronic Supplementary Information (ESI) available: See DOI: 10.1039/x0xx00000x

Physical Chemistry Chemical Physics Accepted Manuscript

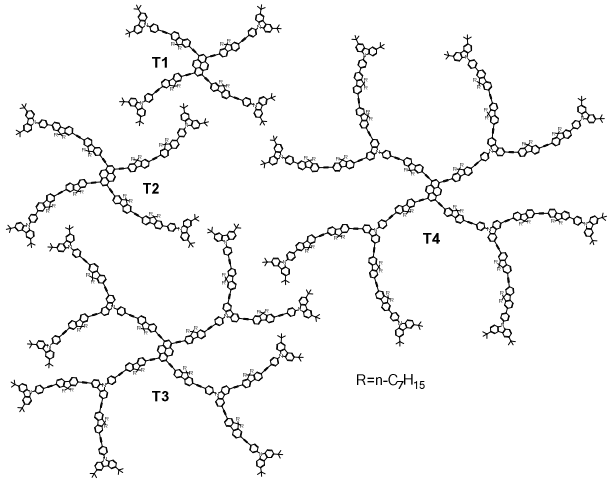

Scheme 1. Molecular Structures of T-series Dendrimers.

2 Computational Methods

2.1 Calculation of One and Two-photon absorption

In the single-beam linearly polarized one color (the angular frequency of ω) 2PA process, the time-dependent wave equation can be described as[44]:

$$\hat{H}\Psi = i\hbar\left(\partial\Psi/\partial t\right) \tag{1}$$

where the Hamiltonian operator is written as:

$$\begin{aligned}\hat{H} &= \hat{H}_0 - \boldsymbol{\mu}\cdot\mathbf{E}_0\cos\omega t \\ &= \hat{H}_0 - e\left|\mathbf{E}_0\right|\left(\mathbf{R}\cdot\boldsymbol{\lambda}\right)\cos\omega t\end{aligned} \tag{2}$$

where $\boldsymbol{\mu}$ is the electronic transition dipole moment and $\mathbf{R}$ is the corresponding spatial vector, $\boldsymbol{\lambda}$ is polarization vector of the radiation, and $\mathbf{E}_0$ is the amplitude vectors of incident sinusoidal electric fields.

According to ref.[45], in the low-temperature case, the 1PA absorption can be written as:

$$\alpha(\omega) = \frac{4\pi^2\omega}{3\hbar c}\left|\boldsymbol{\mu}_{fi}\right|^2\sum_{v'}\left|\left\langle\Theta_{fv'}\middle|\Theta_{i0}\right\rangle\right|^2 D\left(\omega_{fv',i0}-\omega,\gamma_{fv',i0}\right) \tag{3}$$

where $\left|\left\langle\Theta_{fv'}\middle|\Theta_{iv}\right\rangle\right|^2$ is Franck–Condon factor, $D\left(\omega_{fv',i0}-2\omega,\gamma_{fv',i0}\right)$ represents the Lorentzian-shape function, $\boldsymbol{\mu}_{fi}$ is the electronic transition dipole moment between state *f* and state *i*, *v'* is the corresponding vibration quantum numbers of state *f*.

The orientation-averaged 2PA transition rate can be written as

$$\begin{aligned}\left\langle W^{(2)}_{i\to f}(\omega)\right\rangle = &\frac{\pi e^4\left|\mathbf{E}_0\right|^4}{24\hbar^4}\sum_{a}^{x,y,z}\left|\sum_m\frac{\mathbf{R}^a_{fm}\mathbf{R}^a_{mi}}{\omega_{mi}-\omega}\right|^2 \\ &\times\sum_{v'}\left|\left\langle\Theta_{fv'}\middle|\Theta_{i0}\right\rangle\right|^2 D\left(\omega_{fv',i0}-2\omega,\gamma_{fv',i0}\right)\end{aligned} \tag{4}$$

The corresponding 2PA cross section becomes

$$\begin{aligned}\delta_{i\to f}(\omega) = &\frac{16\pi^3\omega^2}{3c\hbar^2}\sum_{a}^{x,y,z}\left|\sum_m\frac{\mathbf{R}^a_{fm}\mathbf{R}^a_{mi}}{\omega_{mi}-\omega}\right|^2 \\ &\times\sum_{v'}\left|\left\langle\Theta_{fv'}\middle|\Theta_{i0}\right\rangle\right|^2 D\left(\omega_{fv',i0}-2\omega,\gamma_{fv',i0}\right)\end{aligned} \tag{5}$$

where *I* is the light intensity,

$$I = \frac{c}{8\pi}\left|\mathbf{E}_0\right|^2 \tag{6}$$

2.2 Calculation of Fluorescence Excitation Anisotropy Spectra

The anisotropy (*r*) was calculated with

$$r = \frac{I_{\parallel}-GI_{\perp}}{I_{\parallel}+2GI_{\perp}} \tag{7}$$

where $I_{\parallel}$ and $I_{\perp}$ are the polarized fluorescence intensities parallel and perpendicular with excitation polarization, respectively; *G* (*G* = $I_{\perp}/I_{\parallel}$) is the geometrical factor of fluorescence spectrophotometer when the excitation is vertically polarized.[8, 46] Furthermore, the angle (β_0) between absorption and emission transition moment can be approximately calculated from corresponding anisotropy (r_0) using equation (8),[47, 48]:

$$r_0 = \frac{2}{5}\left(\frac{3\cos^2\beta_0-1}{2}\right) \tag{8}$$

Anisotropy excitation spectra were calculated according to Equation (7). $I_{//}$ and $I_{\perp}$ are the results of two independent measurements of fluorescence intensity for polarized excitation beams. According to Francesca Terenziani et al's work, $I_{//}$ and $I_{\perp}$ could be calculated efficiently using the following expression[47]:

$$I_{//}(\lambda_{exc},\lambda_{em}) = \frac{1}{15}\sum_{i,j}A_i(\lambda_{exc})F_j(\lambda_{em})\left(1+2\cos^2\theta_{ij}\right) \tag{9}$$

$$I_{\perp}(\lambda_{exc},\lambda_{em}) = \frac{1}{15}\sum_{i,j}A_i(\lambda_{exc})F_j(\lambda_{em})\left(2-\cos^2\theta_{ij}\right) \tag{10}$$

where $A_i(\lambda_{exc})$ is the absorbance from the ground state to the *i*th nonadiabatic excited state at the excitation wavelength λ_{exc}; $F_j(\lambda_{em})$ is the fluorescence intensity from the emitting state towards the *j*th state, the fluorescence wavelength is λ_{em}, θ_{ij} is the angle between the transition dipole moments from ground state to *i*th and *j*th excited states. To calculated excitation anisotropy, $I_{//}(\lambda_{exc},\lambda_{em})$ and $I_{\perp}(\lambda_{exc},\lambda_{em})$ are calculated independently, summed according to the normalized probability and substituted into Eq. (7).

2.3 Computational Methods

In this paper, two-scaled model has been built to determine the optical properties for the T-series dendrimers. For 2 nm scale molecular model for the basic chromophores, the molecular geometries at ground and the excited states were optimized employing B3LYP, CAM-B3LYP and corresponding TD-B3LYP, TD-CAM-B3LYP methods with a basis set of 6-31G(d,p)[23, 49, 50]. Frequency analysis was also carried out at corresponding level. The Huang-Rhys factors at each vibrational mode were also figured out, with which the fluorescence and the absorption band of S_1 have been simulated. Then, for the 10 nm scale model, the ground state geometries of molecules **T1** to **T4** were optimized by using PM6 method. The electronic excited states were computed by ZINDO method with the corresponding ground state optimal conformations. The 1PA and 2PA spectra were calculated using the transition dipole moments obtained from calculation result

Physical Chemistry Chemical Physics Accepted Manuscript

This journal is © The Royal Society of Chemistry 20xx

Please do not adjust margins

of excited states. The excited-state properties of the molecules were also characterized and investigated with the three-dimensional cube representation of the charge difference density (CDD),[8, 51-53] which shows the distribution of net change in electron and hole densities as the results of electronic transitions. The consistency of ZINDO and TD-CAM-B3LYP method was testified. All computations were performed with the Gaussian 09 program package[54].

3 Results and Discussion

3.1. The Molecular Geometry

Core-shell structures are the basic structure feature of stiff T-series dendrimers (**T1**, **T2**, **T3**, and **T4**, shown in **scheme 1**). In all of these dendrimers, pyrene is chosen as the dendrimer core, because of its excellent photoluminescence efficiency (Φ_F=0.60 in cyclohexane)[55, 56]. Fluorenes are chosen as the major chromophores in branches, as their capability of extending the conjugation structure[56]. Carbazoles are chosen as the terminal or the junction chromophores connecting the branches in the first and second generation, since the three- six- and nine- position could be easily modified[57, 58]. Acetylene linkers are chosen as the π-conjugated connection structures of all the chromophores mentioned above[59, 60]. Long alkyl groups would not contribute to the absorption and emission, but they are necessary spacer in dendrimers that prevent the aggregation and self-quenching of nearby chromophores[7, 61]. In a word, the specific dendritic structure is expected to be one of the most remarkable structural motifs for the T-series dendrimers in this article, simultaneously with large 2PA cross section and high TPEF quantum yield[41, 56, 62]. The optical properties of T-series dendrimers are determined by two main chromophores: the polycyclic aromatic pyrene core, and the branch chromophores composed of conjugated fluorene and acetylene (phenylethynyl) linkages combined together. They are the basic structural foundation for the electronic properties.

As a macromolecule, the spatial distribution and the arrangement of chromophores in dendrimers would affect the optical properties significantly. In T-series dendrimers, the number of chromophores is much more than nine, and the distance between two chromophores would not exceed 10 nm. When the dendrimers is excited in light field, the excitation energy transfer and the coupling between chromophores could not be ignored. Moreover, the unique molecular geometry of T-series dendrimers would promote the coupling. In all of these T-series dendrimers, the most obvious character of molecular geometry is the large conjugated planar system which consists of pyrene, fluorene, benzene and the rigid acetylene linkers, and has been reported to be able to increase the π-electron delocalization and enhance the coupling of chromophores among the branches[31, 38, 41, 63]. Furthermore, both the increase of the π-electron delocalization and enhancement of the coupling of chromophores have been reported to be able to enhance the 2PA cross section[31, 38, 41, 63].

In short, the size of T-series dendrimers has far exceeded the range which precise DFT/TD-DFT methods could easily handle. Besides, the T-series dendrimers contain large conjugation sections, and the organization form of the chromophores is not random distribution, and it would inevitably affect the optical properties. Therefore, an overall consideration of multiple chromophores is of crucial importance. Fortunately, the PM6/ZINDO method could be a practical method for such macromolecules system, except that detailed information, such as the information of the molecular structures of the excited states and the vibrational modes, is not available[64, 65]. Combine the advantage of both DFT/TD-DFT and PM6/ZINDO methods, a multi-scaled theoretical investigation was carried out. At 2 nm scale, based on DFT/TD-DFT calculation result, fine molecular models were built for the element chromophores. At 10 nm scale, based on semi-empirical calculation, global models were built for the dendrimers molecules.

3.2. Photophysical Properties of Element Chromophores

In such macromolecule with abundant conjugation sections as T-series dendrimers, chromophores might not be distinctly separated. To build fine molecular models, the element chromophores should be carefully chosen. The proper element chromophores should be able to represent the basic photophysical properties of the global dendrimer significantly. As the primary step, in the molecular models, we divide the dendrimer into two parts with key element chromophores in the branches (**Chromophore B**) and the core (**Chromophore C**) of the T-series dendrimers (shown in **Figure 1**).

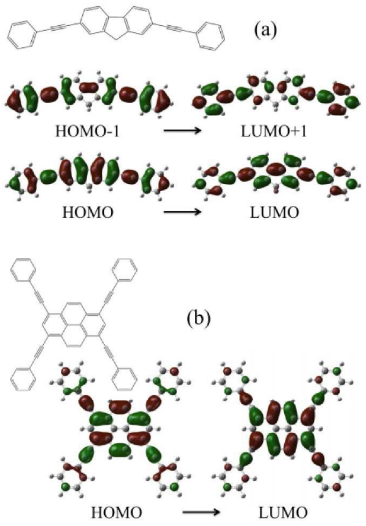

Figure 1. The Molecular Model for (a) **Chromophore B** and (b) **Chromophore C**, and the Corresponding Molecular Orbitals Involved in $S_0 \rightarrow S_1$ Transition.

Physical Chemistry Chemical Physics Accepted Manuscript

Furthermore, in order to give full consideration of the conjugations and linkages among chromophores, not only the acetylene linkers but also benzene rings are included in the models. The HOMOs and LUMOs of the chromophores contribute most to the transition from the ground state (S_0) to the lowest excited singlet state (S_1), which correspond to the absorption (shown in **Figure 1**). The detailed descriptions of the transitions including the molecular orbitals and the corresponding coefficients are listed in the supporting information (**Table S5** and **S6**). The results of different calculation methods are similar to the pattern shown in **Figure1**. The HOMOs are π orbitals distributed on the carbazole or pyrene chromophore and the acetylene linkers, while the LUMOs are the corresponding π* orbitals. The vertical (Franck-Condon) and adiabatic (0-0) transition energies from the ground state to the low-lying singlet states are listed in **Table 1** and **Table 2**. Among them, the adiabatic transitions are more relevant to the measured spectra. The excitation energies of the adiabatic transition obtained by CAM-B3LYP/TD-CAM-B3LYP is 3.28 eV for **Chromophore B**, and 2.48 eV for **Chromophore C,** respectively. It is found that these results are very close to the experimental results[8, 66]. For the semi-empirical method, the optimized structures of the excited states are not available. Therefore, corresponding excitation energies for the adiabatic transition and the precise description of absorption band are yet not available. However, the excitation energies obtained by PM6/ZINDO are 3.32 eV for **Chromophore B**, and 2.59 eV for **Chromophore C**, respectively, which are also very close to the experimental results.

The orbitals and the excitation energies determine the positions of the absorption bands, while the charge distributions and their response to the optical field determine the intensity of the bands. **Figure 2** shows the calculated charge difference densities (CDD), which describe the change in charge distribution as a result of the S_0-S_1 transition as shown in references[8, 51-53]. The electron and hole density contours shown in **Figure 2** agree well with the vacuum molecular orbitals shown in **Figure 1**. The molecular orbitals and the CDD contours indicate that in **Chromophore B** and **C**, the S_0-S_1 transitions belongs to π-π* transition, and that the conjugation structures in **Chromophore B** and **C** are large enough to represent the photophysical properties of the element segment in dendrimers. Moreover, from **Figure 2**, it is found that the calculated CDD contours and the transition dipole moments obtained by TD-CAM-B3LYP calculation agree well with that obtained by ZINDO calculation. It is also found that the CDD contour for the S_0-S_1 transition of **Chromophore C** is very close to that of the T-series dendrimers (shown in **Figure 4 a**). What is more, the CDD contour for the S_0-S_1 transition of **Chromophore B** is also very close to those distributed in the branches of the T-series dendrimers. Taking the consideration of the good agreement of calculated and experimental excitation energies, the reliability of the chosen calculation method could be confirmed, and the consistency of ZINDO and TD-CAM-B3LYP/6-31G(d,p) methods in the system of T-series dendrimers and **Chromophore B** and **C** is also proved.

Table 1. The Excitation Energies for **Chromophore B** and **Chromophore C.**

Excitation Energies (e.V.)	Method	Franck-Condon	Adiabatic
Chromophore B	CAM-B3LYP	3.80180	3.28418
	B3LYP	3.23938	2.89351
	ZINDO	3.31650	
Chromophore C	CAM-B3LYP	2.87067	2.47641
	B3LYP	2.37045	2.15194
	ZINDO	2.59843	

Table 2. The Excitation Energies for T-series dendrimers **T1** to **T4.**

Excitation Energies (e.V.)	Method	Band 1	Band 2
T1	ZINDO	2.49908	3.12981
	Exp.	2.50980	3.16290
T2	ZINDO	2.49450	3.02651
	Exp.	2.50980	3.11520
T3	ZINDO	2.50109	3.11510
	Exp.	2.5098	3.1791
T4	ZINDO	2.50701	3.08672
	Exp.	2.5098	3.0996

Band 1 represent the absorption band in visible spectral region, which correspond to the π-π transition of single chromophore core, **Chromophore C**, while Band 2 represent the absorption band in visible spectral region, which correspond to the π-π* transition of multiple chromophores in branches, **Chromophore B**.

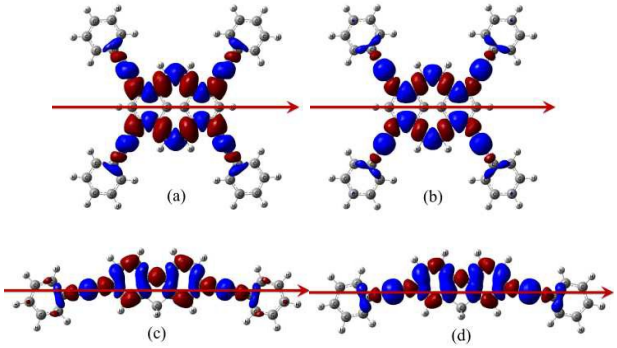

Figure 2. Calculated Excited States Charge Difference density (CDD) of S_0-S_1 transition by (a,c) TD-CAM-B3LYP/6-31G(d,p) and (b,d)ZINDO. The negative density (blue) represents the hole, and the positive density (red) represent the electron. The red arrows represent direction of corresponding transition dipole moments.

Physical Chemistry Chemical Physics Accepted Manuscript

This journal is © The Royal Society of Chemistry 20xx

Please do not adjust margins

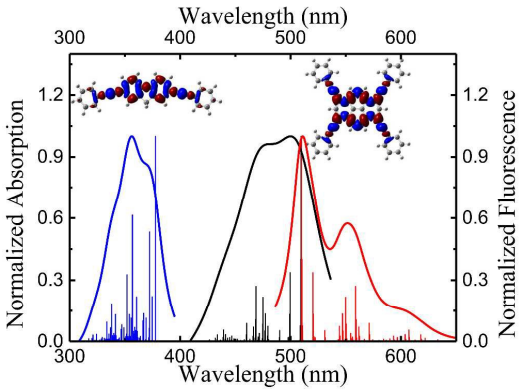

Figure 3. Normalized absorption of **Chromophore B** (blue), Normalized absorption (black) and Fluorescence (red) of **Chromophore C**. To better mimic the detected spectra, Lorentzian line shapes with different FWHMs have been used of absorption and emission bands. For the absorption band, FWHM = 1000 cm^{-1}, and for the emission one FWHM = 500 cm^{-1}.

Based on the optimized structures and vibrational modes of **Chromophore B** and **C**, we have simulated the absorption and fluorescence spectra (shown in **Figure 3**). Vibrational modes and corresponding Huang-Rhys factors are listed in the supporting information (**Table S3** and **S4**). The shape of the S_0-S_1 absorption band of **Chromophore B** is determined by the stretching mode at 1556.7cm^{-1} with a Huang-Rhys factor of 0.61769, which is similar with the reported results in the carbazole system[67, 68]. The simulated S_0-S_1 absorption band of **Chromophore B** is very close to the observed absorption bands of **T1** to **T4** in the 330nm-430nm region[8, 66]. Meanwhile, the stretching mode of **Chromophore C** at 1714cm^{-1} with a Huang-Rhys factor of 0.27436, determines both the shape of S_0-S_1 absorption band and the fluorescence, which is close to the reported results on the pyrene chromophore[69-73]. The simulated S_0-S_1 absorption band (in the 430nm-550nm region) and the fluorescence spectrum of **Chromophore C** are identical with the experimental results of **T1** to **T4** (see **Figure S9** and **S10** in supporting information)[8, 66]. It's very likely that in T-series dendrimers, **Chromophore B** in branches mainly determine the absorption in the 330nm-430nm region, while a single **Chromophore C** in the core determines the absorption in the 430nm-550nm region and the fluorescence.

3.3. The Excited States Distribution and Transition Dipole Moments

The modeling of **T1** to **T4** in 10 nm scale was carried out to obtain an overall understanding of the inter-chromophore effects and energy transfers. Based on the models, the simulated data should be agreed with the experimentally detected ones. As detailed information is not directly available by calculation employing ZINDO method, the molecular models of element chromophores at 2 nm scale were a solid supplement. As mentioned in the previous section, the fine molecular models of element chromophores (**Chromophore B** and **C**) were built, the rationality of the models were testified. As in 2 nm scale, the consistency of calculation result from ZINDO method and TD-DFT method has been testified, the consistency of calculation result at 2 nm and 10 nm by ZINDO calculation has become a crucial factor of the problem.

In visible spectral region, with the identical absorbance and the similar band shape, the absorption bands of **T1** to **T4** are almost the same. According to the calculation, for all of these molecules, only the S_1 state is located in the region above 430 nm. As mentioned in previous sections, the molecular structures of **T1** to **T4** are unique at the core (**Chromophore C**).

CDD contours of the S_0-S_1 transitions in T-series molecules indicate that S_1 states locate mainly in the center chromophores. These CDD contours of **T1** to **T4** are identical not only with each other, but also with the Chromophore C (see **Figure2**, **Figure 4** and **Table S3 S4** in supporting information). The effect of coupling among these chromophores in dendrimers on the optical properties could be quantitatively described in the variation of transition dipole moments. For all the T-series dendrimers from **T1** to **T4**, the S_0-S_1 transition corresponds to the π-π* transition of elections in the pyrene core. As these transitions take place in the identical molecular structure, not only all of the corresponding excitation energies are very close to 2.5 eV, but also all of the amplitude of the corresponding transition dipoles are identical, whose oscillator strength are about ~2.0, with negligible difference. Furthermore, the vibration mode and frequencies are unique for **T1** to **T4**. These characters of molecular structure are further affirmed by the identical fluorescence spectra of **T1** to **T4**.

With excitation energy higher than 2.75 eV, the conjugated fluorene and acetylene in branches would be excited. Different from the region above 430 nm, for the region from 330nm to 430nm, the absorption involves the excitation of several delocalized chromophores (shown in the **Figure 4** and **Table S1** and **S2** in supporting information). As the dendrimer contains large number of conjugated fluorenes and acetylenes, the couplings among them have generated large transition dipole moments. The overall transition dipoles of these chromophores should be taken into consideration so that to describe the S_0-S_x transition and the absorption. From the amplitudes of transition dipoles and oscillator strengths mentioned above, it is also found that the absorptions attributed to the branches is stronger than that attributed to the pyrene core. Besides the overall transition dipoles, the contribution of each chromophore was also marked in the **Figure 4**.

As shown in the **Figure 4 b**, the orientation of the **Chromophore C** center and the overall molecule is not completely overlapped, therefore, there is an angle of about 20° between the overall transition dipole and the minor axis of the **Chromophore C**. Comparing the absorption band of **T1** and **T3** at this region, it is found that the shifting of absorption peaks is insignificant, because the types of chromophores and

Physical Chemistry Chemical Physics Accepted Manuscript

conjugation extent of chromophores in **T1** and **T3** are similar. Meanwhile, as **T3** has one more generation of branches than **T1**, it contains three times the chromophores, the absorption intensity of **T3** is much (about three times) stronger than T1. Comparing the CDD contours of **T1** and **T3** (shown in **Table S1** and **S2** supporting information), it is found that high energy photons (wavelength shorter than 400 nm) are mainly absorbed by chromophores from the outer branches, and therefore, one more generation of branch in the dendrimer would enhance largely the absorption below 400 nm in the spectra.

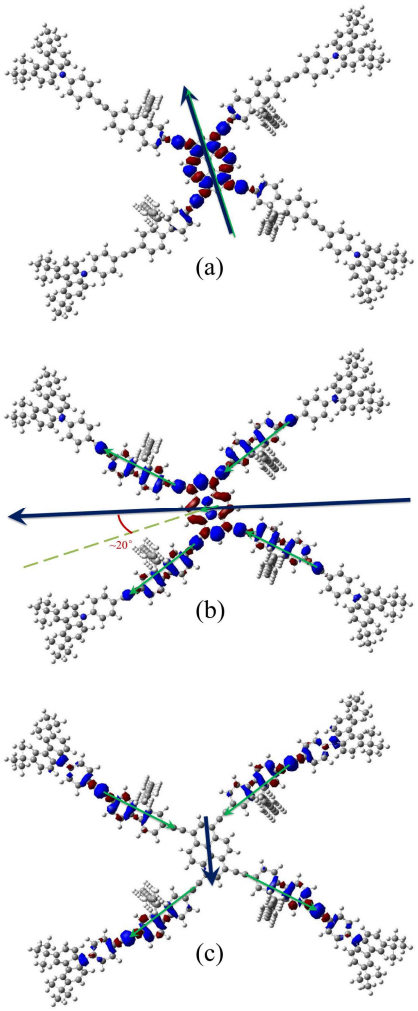

Figure 4. Calculated Excited States Charge Difference density (CDD) of T_1 for Transitions (a)S_0-S_1, (b) S_0-S_4 and (b) S_0-S_6. The negative density (blue) represents the hole, and the positive density (red) represents the electron. The density data shown in this figure were obtained by using ZINDO method. The green arrows represent the transition dipole moments of each individual chromophore and the black ones represent the overall transition dipole moments.

Comparing with the absorption band of **T1**, we find that the absorption band of **T2** is significantly broadened, red-shifted and strengthened. This is because, the conjugation length of the branch chromophores in **T2** is larger than that of **T1**, and the increase of the conjugation length would bring about lower excitation energy, larger delocalization extent of the excited states and larger transition dipole moments, which in turn enhance the intensity of absorptions. Comparing the CDD contours of **T1** and **T2**, it is found that the increase of conjugation length in branches not only enhance the delocalization feature of excited states distribution but also lower the excitation energy. Two extra molecule models were also made: Molecule Model 1 (**M1**, shown in supporting information **Figure S7**) is the **T1** molecule without the ending Carbazole; Molecule Model 2 (**M2**, shown in supporting information **Figure S8**) is the **M1** molecule without the ending benzene ring. Calculation and analysis similar to these done on **T1** to **T4** had been also carried out on M1 and M2, results are show in supporting information (**Figure S11**, **S12** and **Table S7**). Similar to the tendency from **T2** to **T1**, the calculated results from **M1** and **M2** further prove that the reduction in conjugation length causes not only the loss of excited states distribution area but also the blue shift and decrease in the absorption. Similarly, in the case of **T3** and **T4** (shown in **Table S2** supporting information), we find that, even for the second generation branches, it is true that the increase of conjugation length in branches lowers the excitation energy, leading to a broader, more intense, and red-shifted absorption spectra.

Generally, from the CDD contours and the simulated absorption and emission spectra, it is found that the lowest excited state (S_1), from which state the fluorescence is emitted, is localized in the pyrene core, while the excited states with higher energy are delocalized overall chromophores distributed in branches. When the conjugated fluorene and acetylene in branches are excited, the excitation energy would be eventually transferred to the pyrene core before the fluorescence emission as a result of the "antenna effect", and that the "antenna effect" could be largely enhanced by introducing new branches into the molecular system.

3.4. Fluorescence Excitation Anisotropy Spectra.

The feature of 10 nm scale molecular models had been introduced in previous section and the consistency with the 2 nm scale ones is testified. However, to verify the correctness of the 10 nm scale molecular models, quantitative experimental evidence is indispensible. The excitation energies and the transition dipoles among electronic states are two types of such quantitative parameters figured out from the molecular models. Hereon, these data were testified by experimental measurements. Fluorescence excitation anisotropy spectrum is quite sensitive to the change in the transition dipole moments, and hence it's an effective measurement for excitation energy transfer in multi-chromophored system[8, 47, 74-77]. According to equation (8), the angle between absorption and emission could be determined from the fluorescence excitation anisotropy spectra data.

Physical Chemistry Chemical Physics Accepted Manuscript

This journal is © The Royal Society of Chemistry 20xx

Figure 5 shows the calculated fluorescence excitation anisotropy spectra of **T1-T4** , which is in agreement with the experimentally observed fluorescence excitation anisotropy spectra[8].

As shown in **Figure 5**, at the red side of the first absorption band in the region of 430 nm to 550 nm, where the absorption is dominated by the π-π* transition of the only pyrene core, the absorption and emission transition dipoles are unique and parallel, therefore the anisotropy is relatively high (close to 0.4, the theoretical maximum from the Equation (8)). In the region of the second absorption band between 350 nm and430 nm, where the absorption is controlled by numerous chromophores overall the branches, the angle between the absorption and emission transition dipoles is relatively large.

In the case of **T1**, as shown in **Figure 5**, the angle reaches about 70°, therefore, the anisotropy is relatively low down to -0.1. In the region below 350 nm, the anisotropy rises up a little, as the angle between the transition dipole moments of S_0-S_6 and S_0-S_1 is relatively small (as shown in **Figure 5a**). In the case of **T2** to **T4**, the similar trend could be seen (find the data **Table S1** and **S2** in supporting information).

In general, in the region of the first and second absorption bands, the calculated fluorescence excitation anisotropy spectra agree well with the experimental data[8]. It means that not only the amplitude but also the direction could be successfully described, and the calculated transition dipole moments as well as the excitation energy agree with the practical system very well. Unfortunately, due to the lack of consideration of high energy excited states, the simulated spectra deviate from the experimental results at the blue side.

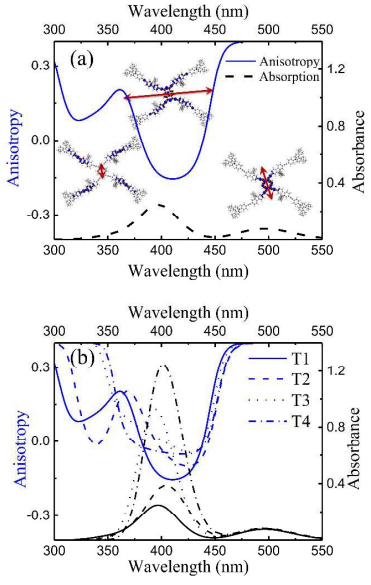

Figure 5. Simulated fluorescence excitation anisotropy spectra (blue) and absorption spectra (black) obtained by ZINDO calculation. (a) The anisotropy spectra and absorption spectra of **T1**. The red arrows represent direction of corresponding transition dipole moments. (b) Comparison of the anisotropy spectra and absorption spectra of **T1** to **T4**.

3.5 Two-Photon Absorption

Hereto, most of the quantitative parameters figured out from the multi-scaled molecular models have been testified by experimental data. The excitation energies were verified by absorption spectra. The molecular structures and vibrational modes were verified by the band-shapes of absorption and emission spectra. The excitation energy distributions and amplitudes and directions of transition dipole moments from ground state to the excited states were verified by the absorption and fluorescence excitation anisotropy spectra. Still, transition dipole moments among excited states are unconfirmed from experimental data. Using the nonlinear optical measures, these data could be solved. To acquire a comprehensive understanding of the system of T-series dendrimers, two-photon absorption (2PA) spectra are simulated to evaluate the transition dipoles among excited states, and testify the molecular model. Furthermore, owing to the potential applications of these dendrimers in three-dimensional microfabrication, photodynamic therapy, high-density optical storage, frequency up-converted lasing, and bio-imaging, the nonlinear optical process of 2PA has rapidly grown into an area of intensive research in the recent decades, and much effort has been made to design and synthesize molecules with high 2PA efficiency[8, 31, 36, 41, 45, 66, 78]. The design and synthesize of the T-series dendrimers is exactly one of these attempts. To further investigate the mechanism how inter-molecular coupling contribute to the enhancement of 2PA cross section, the ground state and the lowest 30 excited states and the transition dipole moments between each two states are taken into consideration, the transition energy and transition dipoles between excited states and ground states are calculated as follows.

From the calculation results of 2PA cross sections by Sum-Over-States method, we found that in the region of 610-850 nm, a three state model covers all of the important contributions. According to equation (**5**) and (6), the main contributions to the 2PA cross sections in the region of 610 nm to 850 nm band (corresponding to the 1PA band from 305 nm to 425nm) are from the term: $\boldsymbol{\mu}_{fm} \cdot \boldsymbol{\mu}_{m0} / (\omega_{m0} - \omega)$, where $\boldsymbol{\mu}_{fm}$ and $\boldsymbol{\mu}_{m0}$ are the transition dipole moments from the state *m* to the final state *f* and the from the ground state to the state *m*, respectively, ω_{m0} is the excitation energy from ground state to the excited state m, and ω is the wavelength of the photon absorbed. To obtain the maximum of $\boldsymbol{\mu}_{fm} \cdot \boldsymbol{\mu}_{m0} / (\omega_{m0} - \omega)$, the state *m* should be S_1 or S_2 so that $\omega_{m0} - \omega$ could reach the minimum, and meanwhile, the transition dipole moments $\boldsymbol{\mu}_{fm}$ and $\boldsymbol{\mu}_{m0}$ should be large and collinear. The dentrimer structures of **T1-T4** make it possible to acquire especially large 2PA cross sections. Firstly, the excitation energy of the S_1 state, which distributed in the pyrene core, is much lower than the other excited states, and therefore the value $\omega_{m0} - \omega$ is considerably reduced, which brings about enhancement in 2PA. Secondly, large conjugation system would promote the charge delocalization, and increase the transition dipole moments, leading to the enlargement of 2PA cross section. Then the cross linked branches bring about more probability for the

Physical Chemistry Chemical Physics Accepted Manuscript

collinear of transition dipole moments, which again enhances the 2PA. Therefore, understanding these structure-properties of dendrimers could be much helpful for synthesis of such kind of photo-functional materials with large TPA cross sections.

Figure 6 shows the two-photon absorption spectra of T-series dendrimers. For comparison, the corresponding one-photon absorption spectra are also shown in **Figure 6**. It is found that in a broad band from 610 nm to 870 nm, these T-series dendrimers have very intensive two-photon absorptions. Since the one-photon and two-photon excitations follow different selection rules, the shapes of 2PA spectrum is quite different from the corresponding 1PA spectrum of the corresponding molecule[8].

As to T-series dendrimers mentioned here, the high energy excited states (with excitation above 3.55 eV) have the most intense 2PA band at around 650nm, and yet, the relatively lower excited states (with excitation 2.88eV to 3.55eV) have the most intense 1PA. Unfortunately, as a result of the lack of consideration of high energy excited states with excitation energies above 3.55 eV, the strong 2PA bands of **T3** and **T4** could not be correctly described, the calculated 2PA spectra of **T3** and **T4** are not included in **Figure 6**.

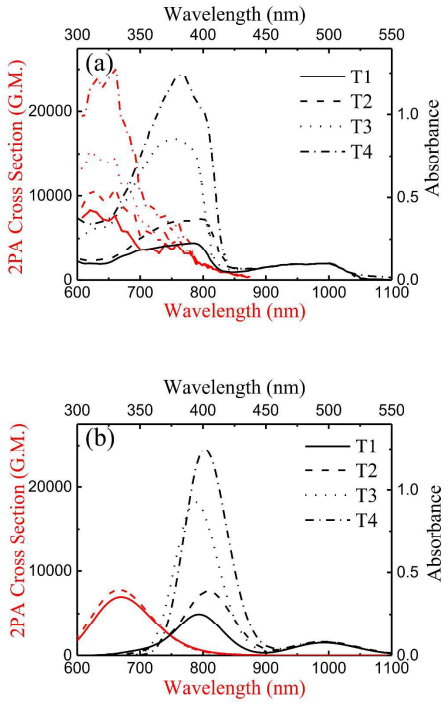

Figure 6. The experimental (a)[8] and simulated (b) two-photon absorption (2PA) spectra (red) of dendrimers. Corresponding 1PA spectra (black) are also shown for comparison.

4 Conclusions

In this work, a practical multi-leveled theoretical investigation is established to determine the structure-related spectral properties for T-series dendrimers based on the proposed molecular model. In 2 nm scale, the molecular models were built for basic chromophores which determine the excitation energies and the absorption and emission band-shapes of the T-series dendrimers. Based on the molecular models and CAM-B3LYP and TD-CAM-B3LYP calculation results, the molecular structures, vibrational properties and electronic densities of these basic chromophores were figured out, and the experiment absorption and emission spectra were successfully reproduced. In 10 nm scale, the overall molecular models were built for dendrimers **T1** to **T4**. ZINDO was employed to simulate electron properties of the whole dendrimers. Based on the molecular models, the experimental data of absorption spectra, fluorescence excitation anisotropy spectra and 2PA spectra were all accurately emulated. Therefore, the correctness of the models was verified. Moreover, the calculation result from 2 nm scale molecular models and those from 10 nm ones aligned fairly well.

As results, the "antenna effect" in the dendrimer molecules are theoretically studied and visualized by using the contour of charge different density (CDD) between electronic states. It is found that the excitation energy is localized from chromophores in branches to the pyrene core before the fluorescence emission. Furthermore, according to the calculation results, it is found that increasing a generation of branches would enhance the absorption with absorption wavelength below 430nm, and enlarging the conjugation of branches would enhance the coupling among the chromophores and lower the excitation energy. The investigation of 2PA spectra also proved that the existence of inter-molecular couplings among the "antenna" chromophores in conjugated branches and the pyrene core would significantly promote two photons absorption. Therefore, these structure-properties of dendrimers explored here could be used as suitable designing strategy for synthesis of advanced materials with large 2PA cross sections. The straight forward strategy as creating a large conjugation plane or adding branches would be helpful in local adjustment, but as the whole spectra from dendrimer, effect of inter-chromophore interactions should be comprehensively considered.

Acknowledgements

This work was supported by the 973 Program (No. 2013CB834604), NSFCs (Nos. 21173235, 21127003, 21333012, and 21373232) and the Strategic Priority Research Program of the Chinese Academy of Sciences (Grant No.XDB12020200).

Notes and references

1. C. Andraud, R. Fortrie, C. Barsu, et al., in *Photoresponsive Polymers Ii*, S.R. Marder and K.S. Lee, Editors. 2008, Springer-

Physical Chemistry Chemical Physics Accepted Manuscript

This journal is © The Royal Society of Chemistry 20xx

Verlag Berlin: Berlin. p. 149.
2. M. Drobizhev, A. Karotki, Y. Dzenis, et al., *J. Phys. Chem. B*, 2003 **107** 7540.
3. M. Drobizhev, A. Karotki, A. Rebane, et al., *Opt. Lett.*, 2001 **26** 1081.
4. Katy A. Green, Peter V. Simpson, T. Christopher Corkery, et al., *Macromol. Rapid Commun.*, 2012 **33** 573.
5. Tzu-Chau Lin, Wei-Lun Lin, Chih-Ming Wang, et al., *Eur. J. Org. Chem.*, 2011 912.
6. Tzu-Chau Lin, Che-Yu Liu, May-Hui Li, et al., *Journal of Materials Chemistry C*, 2014 **2** 821.
7. O. Mongin, T. R. Krishna, M. H. V. Werts, et al., *Chem. Commun.*, 2006 915.
8. Yan Wan, Linyin Yan, Zujin Zhao, et al., *The Journal of Physical Chemistry B*, 2010 **114** 11737.
9. Xiaomei Wang, Feng Jin, Zhigang Chen, et al., *Journal of Physical Chemistry C*, 2011 **115** 776.
10. Bin Xu, Jibo Zhang, Honghua Fang, et al., *Polymer Chemistry*, 2014 **5** 479.
11. Zi-Qi Yan, Bin Xu, Yu-Jie Dong, et al., *Dyes and Pigments*, 2011 **90** 269.
12. T. G. Goodson, *Acc. Chem. Res.*, 2005 **38** 99.
13. Jing Huang, Likai Du, Jun Wang, et al., *Journal of Physical Chemistry C*, 2015 **119** 7578.
14. F. Loiseau, S. Campagna, A. Hameurlaine, et al., *J. Am. Chem. Soc.*, 2005 **127** 11352.
15. Gemma D. D'Ambruoso and Dominic V. McGrath, in *Photoresponsive Polymers Ii*, S.R. Marder and K.S. Lee, Editors. 2008. p. 87.
16. Areej Merhi, Samuel Drouet, Nicolas Kerisit, et al., *Tetrahedron*, 2012 **68** 7901.
17. Zujin Zhao, Juo-Hao Li, Xiaopeng Chen, et al., *J. Org. Chem.*, 2009 **74** 383.
18. Hwan Myung Kim, Cheol Jung, Bo Ra Kim, et al., *Angewandte Chemie-International Edition*, 2007 **46** 3460.
19. Hwan Myung Kim, Bo Ra Kim, Jin Hee Hong, et al., *Angewandte Chemie-International Edition*, 2007 **46** 7445.
20. Hwan Myung Kim, Mun Sik Seo, Myoung Jin An, et al., *Angewandte Chemie-International Edition*, 2008 **47** 5167.
21. T. K. Ahn, K. S. Kim, D. Y. Kim, et al., *J. Am. Chem. Soc.*, 2006 **128** 1700.
22. Ajit Bhaskar, Guda Ramakrishna, Zhikuan Lu, et al., *J. Am. Chem. Soc.*, 2006 **128** 11840.
23. W. H. Lee, H. Lee, J. A. Kim, et al., *J. Am. Chem. Soc.*, 2001 **123** 10658.
24. Alexandre Picot, Anthony D'Aleo, Patrice L. Baldeck, et al., *J. Am. Chem. Soc.*, 2008 **130** 1532.
25. Jeffery E. Raymond, Ajit Bhaskar, Theodore Goodson, et al., *J. Am. Chem. Soc.*, 2008 **130** 17212.
26. M. Rumi, J. E. Ehrlich, A. A. Heikal, et al., *J. Am. Chem. Soc.*, 2000 **122** 9500.
27. Ying Gong, Xunmin Guo, Sufan Wang, et al., *J. Phys. Chem. A*, 2007 **111** 5806.
28. N. Li, K. Jia, S. Wang, et al., *J. Phys. Chem. A*, 2007 **111** 9393.
29. X. N. Ma, L. Y. Yan, X. F. Wang, et al., *PCCP*, 2011 **13** 17273.
30. O. Rubio-Pons, Y. Luo, and H. Agren, *J. Chem. Phys.*, 2006 **124**.
31. Linyin Yan, Xudong Chen, Qingguo He, et al., *The Journal of Physical Chemistry A*, 2012 **116** 8693.
32. F. C. De Schryver, T. Vosch, M. Cotlet, et al., *Acc. Chem. Res.*, 2005 **38** 514.
33. C. Devadoss, P. Bharathi, and J. S. Moore, *J. Am. Chem. Soc.*, 1996 **118** 9635.
34. Mahinda I. Ranasinghe, Oleg P. Varnavski, Jan Pawlas, et al., *J. Am. Chem. Soc.*, 2002 **124** 6520.
35. Damir Aumiler, Sufan Wang, Xudong Chen, et al., *J. Am. Chem. Soc.*, 2009 **131** 5742.
36. D. Beljonne, W. Wenseleers, E. Zojer, et al., *Adv. Funct. Mater.*, 2002 **12** 631.
37. A. S. Davydov, *Soviet Physics Uspekhi*, 1964 **7** 145.
38. Claudine Katan, Francesca Terenziani, Olivier Mongin, et al., *The Journal of Physical Chemistry A*, 2005 **109** 3024.
39. Claudine Katan, Sergei Tretiak, Martinus H. V. Werts, et al., *The Journal of Physical Chemistry B*, 2007 **111** 9468.
40. D. L. Pettit, S. S. H. Wang, K. R. Gee, et al., *Neuron*, 1997 **19** 465.
41. F. Terenziani, C. Katan, E. Badaeva, et al., *Adv. Mater.*, 2008 **20** 4641.
42. F. Terenziani, C. Sissa, and A. Painelli, *J. Phys. Chem. B*, 2008 **112** 5079.
43. T. Yanai, D. P. Tew, and N. C. Handy, *Chem. Phys. Lett.*, 2004 **393** 51.
44. Chih-Kai Lin, Yi-Hsieh Wang, Huan-Cheng Chang, et al., *Journal of Chemical Physics*, 2008 **129**.
45. S.H. Lin. 1984: Academic Press.
46. Joseph R. Lakowicz and Barry R. Masters, *Journal of Biomedical Optics*, 2008 **13** 029901.
47. Cristina Sissa, Anna Painelli, Mireille Blanchard-Desce, et al., *The Journal of Physical Chemistry B*, 2011 **115** 7009.
48. T. J. V. Prazeres, A. Fedorov, S. P. Barbosa, et al., *J. Phys. Chem. A*, 2008 **112** 5034.
49. V. K. Sharma, P. D. Sahare, R. C. Rastogi, et al., *Spectrochimica Acta Part a-Molecular and Biomolecular Spectroscopy*, 2003 **59** 1799.
50. A. D. Becke, *J. Chem. Phys.*, 1993 **98** 5648.
51. M. T. Sun, *J. Chem. Phys.*, 2006 **124**.
52. N. K. Persson, M. T. Sun, P. Kjellberg, et al., *J. Chem. Phys.*, 2005 **123**.
53. X. F. Wang, X. R. Zhang, Y. S. Wu, et al., *Chem. Phys. Lett.*, 2007 **436** 280.
54. Revision D.01 Gaussian 09, M. J. Frisch, G. W. Trucks, H. B. Schlegel, G. E. Scuseria, M. A. Robb, J. R. Cheeseman, G. Scalmani, V. Barone, B. Mennucci, G. A. Petersson, H. Nakatsuji, M. Caricato, X. Li, H. P. Hratchian, A. F. Izmaylov, J. Bloino, G. Zheng, J. L. Sonnenberg, M. Hada, M. Ehara, K. Toyota, R. Fukuda, J. Hasegawa, M. Ishida, T. Nakajima, Y. Honda, O. Kitao, H. Nakai, T. Vreven, J. A. Montgomery, Jr., J. E. Peralta, F. Ogliaro, M. Bearpark, J. J. Heyd, E. Brothers, K. N. Kudin, V. N. Staroverov, R. Kobayashi, J. Normand, K. Raghavachari, A. Rendell, J. C. Burant, S. S. Iyengar, J. Tomasi, M. Cossi, N. Rega, J. M. Millam, M. Klene, J. E. Knox, J. B. Cross, V. Bakken, C. Adamo, J. Jaramillo, R. Gomperts, R. E. Stratmann, O. Yazyev, A. J. Austin, R. Cammi, C. Pomelli, J. W. Ochterski, R. L. Martin, K. Morokuma, V. G. Zakrzewski, G. A. Voth, P. Salvador, J. J. Dannenberg, S. Dapprich, A. D. Daniels, Ö. Farkas, J. B. Foresman, J. V. Ortiz, J. Cioslowski, and D. J. Fox, Gaussian, Inc., Wallingford CT, 2009.
55. P. C. Bevilacqua, R. Kierzek, K. A. Johnson, et al., *Science*, 1992 **258** 1355.
56. Hwan Myung Kim and Bong Rae Cho, *Chem. Commun.*, 2009 153.
57. Zujin Zhao, Xinjun Xu, Xiaopeng Chen, et al., *Tetrahedron*, 2008 **64** 2658.
58. O. K. Kim, K. S. Lee, H. Y. Woo, et al., *Chem. Mater.*, 2000 **12** 284.
59. T. H. Huang, Y. J. Chen, S. S. Lo, et al., *Dalton Transactions*, 2006 2207.
60. Hwan Myting Kim, Bo Ra Kim, Myoung Jin An, et al., *Chemistry-a European Journal*, 2008 **14** 2075.
61. Olivier Mongin, Anna Pla-Quintana, Francesca Terenziani, et al., *New J. Chem.*, 2007 **31** 1354.
62. Guang S. He, Loon-Seng Tan, Qingdong Zheng, et al., *Chem. Rev.*, 2008 **108** 1245.
63. F. Terenziani, C. Le Droumaguet, C. Katan, et al., *Chemphyschem*, 2007 **8** 723.
64. M. A. Thompson and M. C. Zerner, *J. Am. Chem. Soc.*, 1991 **113** 8210.
65. James J. P. Stewart, *J. Mol. Model.*, 2007 **13** 1173.
66. Z. J. Zhao, J. H. Li, X. P. Chen, et al., *J. Org. Chem.*, 2009 **74** 383.
67. Duy Duc Nguyen, John Trunk, Lina Nakhimovsky, et al., *Journal*

Physical Chemistry Chemical Physics Accepted Manuscript

of Molecular Spectroscopy, 2010 **264** 19.
68. N. A. Borisevich, V. A. Povedailo, and D. L. Yakovlev, *Optics and Spectroscopy*, 2006 **100** 351.
69. K. Kalyanasundaram and J. K. Thomas, *J. Am. Chem. Soc.*, 1977 **99** 2039.
70. A. Nakajima, *I. Mol. Spectrosc.*, 1976 **61** 467.
71. G. Marconi and P. R. Salvi, *Chem. Phys. Lett.*, 1986 **123** 254.
72. D. S. Karpovich and G. J. Blanchard, *J. Phys. Chem.*, 1995 **99** 3951.
73. V. G. Avakyan, V. B. Nazarov, A. V. Koshkin, et al., *High Energ. Chem.*, 2015 **49** 177.
74. Steven S. Andrews, *J. Chem. Educ.*, 2004 **81** 877.
75. Xunmin Guo, Sufan Wang, Andong Xia, et al., *J. Phys. Chem. A*, 2007 **111** 5800.
76. Mingli Jia, Xiaonan Ma, Linyin Yan, et al., *J. Phys. Chem. A*, 2010 **114** 7345.
77. Telmo J. V. Prazeres, Alexander Fedorov, Sandrina P. Barbosa, et al., *The Journal of Physical Chemistry A*, 2008 **112** 5034.
78. Marius Albota, David Beljonne, Jean-Luc Brédas, et al., *Science*, 1998 **281** 1653.

TOC Graphic

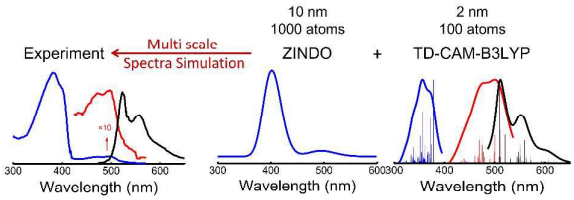

Multi-scale theoretical model and spectra simulation for dendrimers combining TD-DFT/DFT and semi-empirical methods.

Physical Chemistry Chemical Physics Accepted Manuscript

This journal is © The Royal Society of Chemistry 20xx